Structural transitions in the two-dimensional Jahn-Teller system $K_2Cu_xZn_{1-x}F_4$ with the variation of x: experiments based on the Raman scattering of phonons

1991 J. Phys.: Condens. Matter 3 6925

(http://iopscience.iop.org/0953-8984/3/35/022)

J. Phys.: Condens. Matter 3 (1991) 6925–6933. Printed in the UK

Structural transitions in the two-dimensional Jahn–Teller system $K_2Cu_xZn_{1-x}F_4$ with the variation of x: experiments based on the Raman scattering of phonons

Y Fukada, M Totani and I Yamada
Department of Physics, Faculty of Science, Chiba University, Yayoi-cho, Chiba-260, Japan

Received 18 March 1991

Abstract. Measurements are reported of the Raman scattering of phonons in many crystals of $K_2Cu_xZn_{1-x}F_4$ with different Cu concentrations x. With decreasing x, a structural change is confirmed at $x \sim 0.8$ besides the one at $x \sim 0.4$. Comparing the observed polarized spectra for $1 \geqslant x > 0.8$ with those for $0.8 > x > 0.4$, we find a transition at $x \sim 0.8$ from the D_{2h} to an apparent D_{4h} symmetry, which corresponds to a change of the long-range order of the cooperative Jahn–Teller distortion of CuF_6 octahedra from three-dimensional to two-dimensional. Below $x \sim 0.4$, the long-range antiferrodistortive order in each c plane is destroyed as reported by Natsume and Yamada (NY) in 1985. The observed Stokes line including several lines which were missed in the report by NY for $x > 0.8$, $0.8 > x > 0.4$ and $0.4 > x$ are well explained on the assumption of the space groups of D_{2h}^{18}, D_{4h}^{5} and D_{4h}^{17}, respectively.

1. Introduction

Measuring the phonon Raman scattering, we have confirmed [1] that the crystal structure of the well known cooperative Jahn–Teller system K_2CuF_4 is assigned to the space group of D_{2h}^{18}. The D_{2h} or the twofold symmetry around the c axis comes entirely from the three-dimensional correlation of the lattice distortion. In other words, a regular stacking of the c planes in which CuF_6 octahedra order antiferrodistortively, constructs the twofold symmetry which is uncommon in the compounds with a K_2NiF_4-type structure because they have a fourfold symmetry around the c axis. The D_{2h} point symmetry indicates that the antiferrodistortive order of CuF_6 octahedra in each c plane is correlated with that in the nearest-neighbour c planes. Hence we can say that the D_{2h} symmetry arises from the three-dimensional order of the distortion of CuF_6. The coupling between the adjacent c planes is, however, very weak and it can be neglected in some cases. When neglected, an adequate space group should be D_{4h}^{5} as has been reasonably adopted in several studies [2–6] on this compound. For instance, Riley *et al* [5] employed D_{4h}^{5} in their analysis of the optical measurements of absorption, magnetic circular dichroism and Zeeman spectra, considering that the electronic transitions are localized mainly in a single Cu^{2+} ion.

Basing our study on the fact that K_2CuF_4 has the distortive order not only in the c plane but also along the c axis, we have investigated the effect of dilution by Zn^{2+} ions on the three-dimensional distortive order mentioned above. In the early paper [4], a study of the phonon Raman scattering for $K_2Cu_xZn_{1-x}F_4$ (abbreviated to Cu–Zn from now on) was reported and was discussed successfully from the point of view

0953-8984/91/356925+09$03.50

of percolation phenomena for the two-dimensional order. However, the experiment in that study was done only at room temperature and several further Stokes lines which should appear on the polarized spectra were missed even for $x = 1$ and $x = 0$. Moreover, the samples were not examined with due regard to the domain structures [1,9]. Such insufficient results have urged us to study Cu–Zn further. As a result of the present experiments, we have found that an additional structural transition occurs at $x \sim 0.8$ besides the one at $x \sim 0.4$ reported earlier [4]. We shall develop our experimental results and discuss them in the following section.

2. Experimental results and discussion

We have prepared more than ten samples with different x by cutting sections from single crystals which were grown by the Bridgman method [7,8]. They were shaped into rectangular parallelepipeds of about $4 \times 4 \times 4$ to $10 \times 5 \times 5$ mm^3 sizes with the faces of $(001)_p$, $(110)_p$ and their equivalents, where $(\ )_p$ indicates a plane in a K_2NiF_4-type structure. The unevenness of the polished surfaces was 5–10 μm. All the spectra were obtained at 10 K at which the widths of the Stokes lines were very much smaller than those observed at room temperature and hence lines in close proximity to each other were more distinguishable. Because of the almost complete transparency of Cu–Zn crystals to visible light, there was no problem of self-heating of the samples for incident light of the 514.5 nm polarized line of an argon laser with power of about 100–200 mW. We have employed a 90° scattering geometry for the same Raman spectrometer as has been introduced previously [1]. The laboratory axes X, Y and Z which are necessary to indicate the polarization of incident and scattered light are defined in [1]; i.e., in principle, $X \| [110]_p$, $Y \| [1\bar{1}0]_p$ and $Z \| [001]_p$.

Before developing the present result for $x < 1$, we briefly summarize the report [1] in which the experiments and the analysis for $x = 1$ is given. The Stokes line which appeared in the polarized spectra for $x = 1$ are well assigned to the normal modes derived from the D_{2h}^{18} space group; the Raman-active modes are

$$4A_g + 4B_{1g} + 5B_{2g} + 5B_{3g}.$$

Then 18 Stokes lines are expected and among them 16 Stokes lines were confirmed in the polarized spectra [1]†. The most explicit evidence of the D_{2h} or the twofold symmetry appears as the difference between the ZX and ZY spectra in which the Stokes lines are assigned to the B_{2g} and B_{3g} modes, respectively.

With decreasing x in Cu–Zn, however, the ZX and ZY spectra begin to coincide with each other around $x \sim 0.8$ and then the number of the Stokes lines decreases substantially. When x is decreased further, several Stokes lines in the XX, ZZ, XY, ZX and ZY spectra lose their scattering intensity and disappear around $x \sim 0.4$ and only four lines remain for $x < 0.4$. These circumstances can be seen in figure 1 which represents the variation of the vibrational energies of the observed Stokes lines

† We reported in [1] that 17 Stokes lines were found in the polarized spectra, but after the paper [1] was published, we confirmed that the line 5^s appearing in the XY spectrum represented a 'leakage' of the strong line 6^s that was observed in the XX spectrum; the leakage was caused by the separation between the directions of X and the normal of the surface exposed to the incident light. As a result, 16 lines among 18 lines expected theoretically are confirmed, though this fact has no effect on our proposal of the D_{2h}^{18} symmetry for K_2CuF_4.

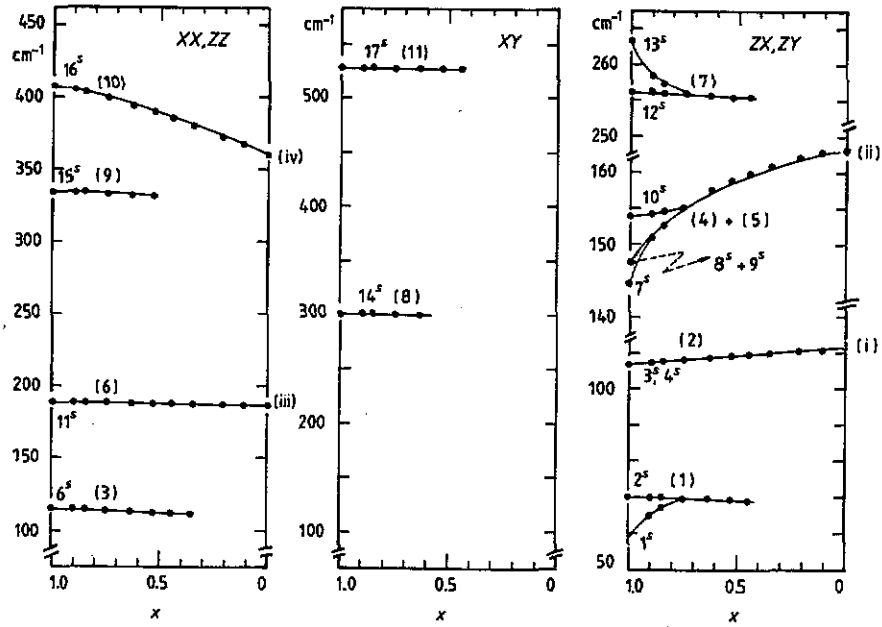

Figure 1. Dependence of the energy (the Stokes shift) of the Stokes lines on the variation of x in $K_2Cu_xZn_{1-x}F_4$ observed at 10 K in the polarized spectra of XX, ZZ, XY, ZX and ZY. the numbers 1^s–16^s for $x = 1$, (1)–(11) for $x = 0.75$ and (i)–(iv) for $x = 0$ are attached. The full curves are drawn as a guide to the eye.

with x. In this figure, we attach the numbers 1^s–16^s to the positions of the lines for $x = 1$ following [1], (1)–(11) for $x = 0.75$ and (i)–(iv) for $x = 0$, which will be convenient for discussion.

To see the change around $x \sim 0.8$ mentioned above, we show the ZX and ZY spectra for several samples with x around 0.8 in figure 2. We find that several pairs of lines observed for $x = 1$—a counterpart of each pair appears independently in the ZX and ZY spectra—converge into single lines when x become lower than 0.8, which is easily understood when we see the (Z_Y^X) spectra. As shown in figure 2(a) for example, the counterparts 1^s and 2^s for $x = 1$ are independently observed in the ZX and ZY spectra, and they still appear separately for $x = 0.85$. However, they converge into the line numbered (1) for $x = 0.75$ which appears at the same positions in the ZX and ZY spectra. Such a coincidence of the ZX and ZY spectra indicates that the apparent crystal symmetry loses the D_{2h} character and instead becomes of D_{4h} or fourfold character, which arises from the destruction of the correlation of the distortion among the adjacent c planes caused by the random displacement of Cu by Zn. Only the counterparts 3^s and 4^s are exceptions, i.e., they appear at the same positions regardless of the variation of x. As suggested in [1] and as will be clarified below, the normal modes corresponding to these two lines are the vibrations of the K atoms and hence their energies are almost irrelevant to both the cooperative distortion of CuF_6 and the displacement of Cu by Zn.

A randomly site diluted crystal, of course, has no periodic arrangement of atoms, and therefore, properly speaking, it is impossible to assign a space group to such a system. To discuss experiments such as x-ray diffraction, optical scattering etc., made on a randomly diluted or mixed crystal, however, it is convenient to assume a certain space group as the present case. All polarized spectra for $x = 0.75$ representing

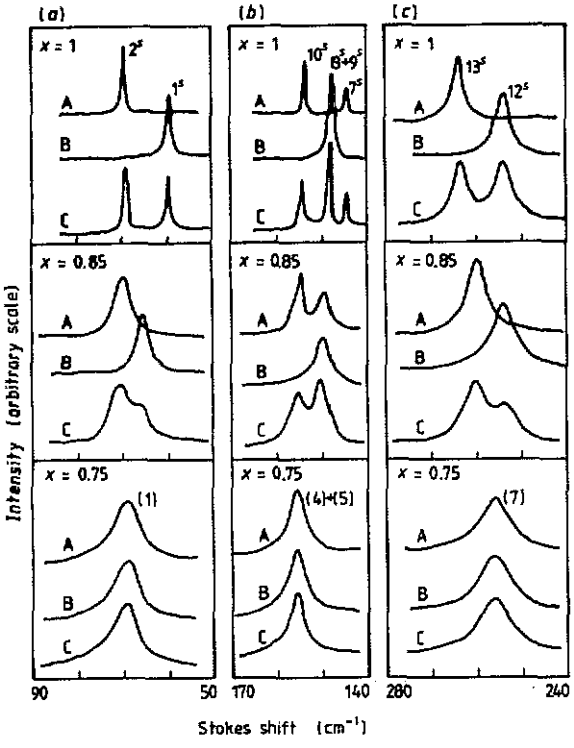

Figure 2. Change of the ZX and ZY spectra with x around $x \sim 0.8$; the lines denoted A are ones in the ZY, B in the ZX and C in the (Z_Y^X) spectra. The attached numbers 1^s, 2^s... and (1), (4) + (5)... are explained in the text. The (Z_Y^X) spectra were taken by removing the analyser to confirm whether or not the ZX and ZY spectra coincide with each other.

those for $0.8 > x > 0.4$ are shown in figure 3 which should be compared with the spectra for $x = 1$ given as the figures 3 and 4 in [1]. Assuming the D_{4h}^5 space group, let us analyse the data for $x = 0.75$. The Raman-active modes for D_{4h}^5 expressed following the notation for the D_{4h} point group are

$$3A_{1g} + B_{1g} + 3B_{2g} + 5E_g$$

in which the E_g mode is doubly degenerate. Their Raman tensors are

$$A_{1g} = \begin{pmatrix} a & 0 & 0 \\ 0 & a & 0 \\ 0 & 0 & b \end{pmatrix} \qquad B_{1g} = \begin{pmatrix} c & 0 & 0 \\ 0 & -c & 0 \\ 0 & 0 & 0 \end{pmatrix} \qquad B_{2g} = \begin{pmatrix} 0 & d & 0 \\ d & 0 & 0 \\ 0 & 0 & 0 \end{pmatrix}$$

$$E_g = \begin{pmatrix} 0 & 0 & e \\ 0 & 0 & 0 \\ e & 0 & 0 \end{pmatrix} \qquad \text{and} \qquad \begin{pmatrix} 0 & 0 & 0 \\ 0 & 0 & e \\ 0 & e & 0 \end{pmatrix}.$$

We can then expect Stokes lines as follows: three lines of A_{1g} and a line of B_{1g} in the XX $(= YY)$; three lines of A_{1g} in the ZZ; three lines of B_{2g} in the XY; five lines of E_g in the ZX $(= ZY)$ spectrum. As can be seen in figure 3, three lines numbered (6), (9) and (10) are distinguished in the ZZ spectrum for $x = 0.75$ and hence they are of A_{1g} character. The lines (9) and (10) also appear in the XX spectrum, while the line (6) does not. Instead, a strong line (2) appears in the XX spectrum. As a consequence, we assign the lines (6), (9) and (10) to A_{1g} and the line (2) to B_{1g}. Though three lines are predicted in the XY spectrum, only two lines (8)

and (11) are confirmed and they are hence inevitably of B_{2g} character. On the other hand, we find that the ZX spectrum for $x = 0.75$ involving four lines coincides well with the ZY spectrum, indicating a fourfold symmetry. Then we can recognize that the lines in the ZX $(= ZY)$ spectrum are yielded as a result of the degeneracy of B_{2g} and B_{3g} in the D_{2h} symmetry with E_g in the D_{4h} symmetry. On the face of it, one line is missing in the ZX $(= ZY)$ spectrum because the theory suggests five lines. We think, however, that the doubly numbered line $(4) + (5)$, the intensity of which is apparently very strong, consists of two lines, (4) and (5), as explained for the line numbered $8^s + 9^s$ for $x = 1$ [1].

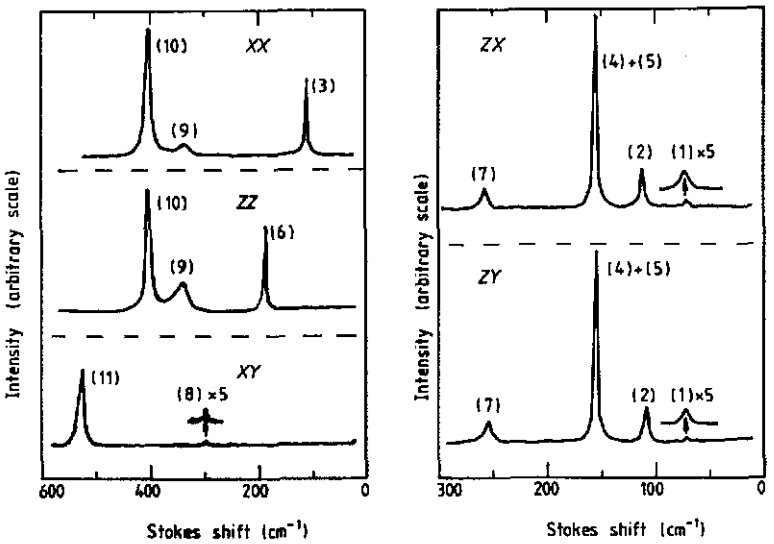

Figure 3. Polarized spectra for $K_2Cu_xZn_{1-x}F_4$ with $x = 0.75$ which represent the results for $0.8 > x > 0.4$. The observed Stokes lines are numbered as (1)–(11) for the convenience of discussion.

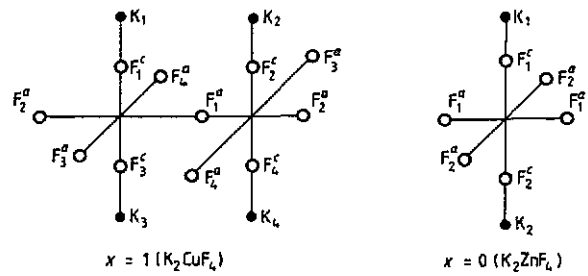

Figure 4. Group of atoms necessary to show the symmetry adapted vectors (SAV) which are given in table 2. Since the unit cell of K_2CuF_4 $(x = 1)$ contains two molecules, the adjacent two molecules are shown. The subscript numbers attached to the respective atoms are referred to when the SAVs are defined and F^a and F^c indicate the F atoms in the c plane and on the c axis, respectively. The Cu or Zn atom locates at the centre of the F octahedron, but both of them are omitted.

As discussed above, the spectra for $x = 0.75$ representing $0.8 > x > 0.4$ are well explained on the assumption of the D_{4h}^5 space group, which indicates the distortive

order being completely two-dimensional as a result of disappearance of the correlation of the distortion among the adjacent c planes. The present result corresponds to the phenomena observed in the x-ray diffraction patterns for Cu–Zn around $x \sim 0.8$ reported by Hidaka *et al* in [9]. That is, they confirmed that the spot-like superlattice reflections for $x > 0.8$ turn into the rod-like ones below $x \sim 0.8$. This indicates a change of the long-range order of the distortion of CuF_6 from three-dimensional to two-dimensional.

The change of the spectra round $x \sim 0.4$ can be explained from the point of view of the two-dimensional percolation phenomena as discussed earlier [4]. That is, the distortive long-range order in each c plane persists well below the percolation threshold $x_c(1) = 0.59$ for the first-nearest-neighbour coupling on the square lattice. Rather, it remains down to $x \sim 0.4$ which is close to the second percolation threshold $x_c(1,2) = 0.41$ for the first- and the second-nearest-neighbour couplings on the square lattice.

The four lines observed below $x \sim 0.4$ are explained on the assumption of the D_{4h}^{17} space group which is assigned to K_2ZnF_4, i.e., $x = 0$. As clarified in many studies, the compounds of K_2MF_4 in which MF_6 octahedra have no distortion involve the Raman-active modes as

$$2A_{1g} + 2E_g$$

and then Stokes lines are expected in the spectra as follows: two lines of A_{1g} in the XX $(= YY)$ and ZZ spectra; two lines of E_g in the ZX $(= ZY)$ spectra. From the experimental results shown in figure 1, we assign the lines numbered (iii) and (iv) to A_{1g}, and the lines (i) and (ii) to E_g.

Strictly speaking, we have found that the sample with $x = 0.35$ still shows very weak Stokes lines relevant to the two-dimensional distorted order. We think that the sample with $x = 0.35$ has finite but very large CuF_6 clusters the sizes of which are comparable to, or longer than, the wavelength of the incident light. In such large finite clusters, the distortion of CuF_6 should still be cooperative similarly to the case for $0.8 > x > 0.4$ as suggested in the EPR study on Cu–Zn [8] and hence the appearance of the Stokes lines for $x = 0.35$ referred to above is reasonably understood. Anyway, the change of the spectra around $x \sim 0.4$ corresponds to the collapse of the two-dimensional distortive long-range order.

The correspondence of the normal modes for D_{2h}^{18}, D_{4h}^{5} and D_{4h}^{17} is given in table 1. We shall now show the approximate vibrational form or the eigenvectors of each mode for $x = 1$ and $x = 0$ and shall justify the correspondence given in table 1. To determine the energies and eigenvectors, group theory is used to find symmetry-adapted vectors (SAVs) and the dynamical matrix is solved algebraically on the basis of the rigid-ion model. The SAVs for the predicted lattice vibrations have been constructed following the method explained in the conventional texts of group theory and its application. The SAVs thus obtained are given in table 2 in which $Q^{\alpha}(j)$ denotes a SAV of one of the modes given by an irreducible representation α such as A_g, B_{1g}, etc. We indicate the atoms relevant to the vectors following the definition given in figure 4. When more than one normal mode transforms as a given irreducible representation, the normal modes are distinguished from each other by a number (j). The eigenvector $e^{\alpha}(i)$ can be given by a linear combination of $Q^{\alpha}(j)$. In the calculation of the dynamical matrix, we have used several parameters of the potentials or the force constants F–F, K–K, F–K and Zn–F given in [10–14]

Table 1. Correspondence of the normal modes among the three space groups D_{2h}^{18}, D_{4h}^{5} and D_{4h}^{17}. The numbers attached to the observed lines for $x = 1$ (1^s, 2^s, ...), $x = 0.75$ ((1), (2), ...) and $x = 0$ ((i), (ii), ...) are also shown.

D_{2h}^{18}			D_{4h}^{5}			D_{4h}^{17}	
$A_g(1)$;	15^s	⟷	$A_{1g}(1)$;	(9)			
$A_g(2)$;	6^s	⟷	B_{1g};	(3)			
$A_g(3)$;	16^s	⟷	$A_{1g}(2)$;	(10)	⟷	$A_{1g}(1)$;	(iv)
$A_g(4)$;	11^s	⟷	$A_{1g}(3)$;	(6)	⟷	$A_{1g}(2)$;	(iii)
$B_{1g}(1)$;	17^s	⟷	$B_{2g}(1)$;	(11)			
$B_{1g}(2)$;	missed	⟷	A_{2g};	inactive			
$B_{1g}(3)$;	14^s	⟷	$B_{2g}(2)$;	(8)			
$B_{1g}(4)$;	missed	⟷	$B_{2g}(3)$;	missed			
$B_{2g}(1)$; $B_{3g}(1)$;	12^s 13^s	⟷	$E_g(1)$;	(7)			
$B_{2g}(2)$; $B_{3g}(2)$;	8^s 7^s	⟷	$E_g(2)$;	(4) or (5)	⟷	$E_g(1)$;	(ii)
$B_{2g}(3)$; $B_{3g}(3)$;	1^s 2^s	⟷	$E_g(3)$;	(1)			
$B_{2g}(4)$; $B_{3g}(4)$;	3^s 4^s	⟷	$E_g(4)$;	(2)	⟷	$E_g(2)$;	(i)
$B_{2g}(5)$; $B_{3g}(5)$;	9^s 10^s	⟷	$E_g(5)$;	(4) or (5)			

and have treated the force constants for long and short Cu-F distances as adjustable parameters. The approximate eigenvectors thus determined for $x = 1$ and $x = 0$, but for the arbitrary disposal of the mass-weighted normalization, are given in table 2, which is helpful for understanding the correspondence given in table 1.

As can be understood from table 2, the direction of the displacements of the F or K atoms in the counterparts $B_{2g}(i)$ and $B_{3g}(i)$ ($i = 1$–5) are orthogonal to each other. When the respective counterparts $B_{2g}(i)$ and $B_{3g}(i)$ degenerate, the restriction for the direction of the displacements in the c plane is lifted, and then they converge into $E_g(i)$ ($i = 1$–5), which appears as the change of the ZX and ZY spectra around $x = 0.8$.

The transition around $x \sim 0.4$ is described [4] as a result of an expansion of the Brillouin zone that brings about a shift of several modes from a Γ point considered in the D_{4h}^5 structure towards an M point in the D_{4h}^{17} structure. Since only the vibrations at the Γ points are detected by Raman scattering, the normal modes irrelevant to such a change of the Brillouin zone survive as Raman-active down to $x = 0$. Such a circumstance is understood when we compare the vibrational form of, for instance, $B_{2g}(4)$ with that of $B_{2g}(5)$. The vibrations of $B_{2g}(4)$ and $B_{2g}(5)$ involve displacement of the K atoms. In the former mode, the sense of the displacements in adjacent molecules is identical, while in the latter mode, the displacements have opposite sense. Then the vibrations of $B_{2g}(4)$ are not concerned with the change of the Brillouin zone mentioned above. As a consequence, the correspondence of the normal modes given in table 1 is supported, though the eigenvectors are derived from the approximate calculation.

Before we conclude our discussion, let us add the following. We have found very weak and broad extra lines for $x = 0.02$–0.1 at 40–50 cm^{-1} which are absent in

Table 2. Symmetry-adapted vectors $Q^{\alpha}(j)$ and the approximate eigenvectors $e^{\alpha}(i)$ for the zone centre modes. To construct $e^{\alpha}(i)$ as a linear combination of $Q^{\alpha}(j)$, minor terms are omitted. The superscript α indicating an irreducible representation such as A_g, B_{1g} and so on is omitted for convenience. The atoms relevant to the displacements are given on the right side of the vectors $Q^{\alpha}(j)$; F^a and F^c indicate the F atoms in the c plane and on the c axis, respectively. The subscripts of the coordinates 1, 2, 3 and 4 refer to the atoms participating in each mode as shown in figure 4. The coordinate system $[xyz]$ is chosen so as to have z parallel to $[001]_p$, while x and y are parallel to $[100]_p$ and $[010]_p$, respectively, where $[\ ]_p$ indicates a direction in the unit cell of a K_2NiF_4-type structure. The origin is chosen to be the position of the Cu or Zn atom. The coefficients a_i and b_i ($i = 1$–3) of the combinations of $Q^{\alpha}(j)$ are 0.5–0.8.

α	$Q^{\alpha}(j)$		$e^{\alpha}(i)$
$x = 0$ (K_2ZnF_4)			
$A_{1g}(1)$:	$Q(1) = z_1 - z_2$	F^c	$e(1) \sim Q(1)$
$A_{1g}(2)$:	$Q(2) = z_1 - z_2$	K	$e(2) \sim Q(2)$
$E_g(1)$:	$Q(1) = x_1 - x_2$ (or $y_1 - y_2$)	F^c	$e(1) \sim Q(1)$
$E_g(2)$:	$Q(2) = x_1 - x_2$ (or $y_1 - y_2$)	K	$e(2) \sim Q(2)$
$x = 1$ (K_2CuF_4)			
$A_g(1)$:	$Q(1) = -y_1 + y_2 + x_3 - x_4$	F^a	$e(1) \sim Q(1)$
$A_g(2)$:	$Q(2) = -x_1 + x_2 + y_3 - y_4$	F^a	$e(2) \sim Q(2)$
$A_g(3)$:	$Q(3) = x_1 + x_2 - z_3 - z_4$	F^c	$e(3) \sim Q(3)$
$A_g(4)$:	$Q(4) = x_1 + x_2 - z_3 - z_4$	K	$e(4) \sim Q(4)$
$B_{1g}(1)$:	$Q(1) = -y_1 + y_2 - x_3 + x_4$	F^a	$e(1) \sim a_1Q(1) - b_1Q(3)$
$B_{1g}(2)$:	$Q(2) = x_1 - x_2 + y_3 - y_4$	F^a	$e(2) \sim Q(2)$
$B_{1g}(3)$:	$Q(3) = x_1 - x_2 - z_3 + z_4$	F^c	$e(3) \sim a_1Q(1) + b_1Q(3)$
$B_{1g}(4)$:	$Q(4) = x_1 - x_2 - z_3 + z_4$	K	$e(4) \sim Q(4)$
$B_{2g}(1)$:	$Q(1) = -x_1 + z_2 + z_3 - z_4$	F^a	$e(1) \sim a_2Q(1) - b_2Q(3)$
$B_{2g}(2)$:	$Q(2) = \frac{1}{\sqrt{2}}[(x_1 + y_1) + (x_2 + y_2) + (-x_3 - y_3) + (-x_4 - y_4)]$	F^c	$e(2) \sim Q(2)$
$B_{2g}(3)$:	$Q(3) = \frac{1}{\sqrt{2}}[(-x_1 + y_1) + (x_2 - y_2) + (x_3 - y_3) + (-x_4 + y_4)]$	F^c	$e(3) \sim a_2Q(1) + b_2Q(3)$
$B_{2g}(4)$:	$Q(4) = \frac{1}{\sqrt{2}}[(x_1 + y_1) + (x_2 + y_2) + (-x_3 - y_3) + (-x_4 - y_4)]$	K	$e(4) \sim Q(4)$
$B_{2g}(5)$:	$Q(5) = \frac{1}{\sqrt{2}}[(-x_1 + y_1) + (x_2 - y_2) + (x_3 - y_3) + (-x_4 + y_4)]$	K	$e(5) \sim Q(5)$
$B_{3g}(1)$:	$Q(1) = -x_1 + x_2 - z_3 + z_4$	F^a	$e(1) \sim a_3Q(1) + b_3Q(3)$
$B_{3g}(2)$:	$Q(2) = \frac{1}{\sqrt{2}}[(x_1 - y_1) + (x_2 - y_2) + (-x_3 + y_3) + (-x_4 + y_4)]$	F^c	$e(2) \sim Q(2)$
$B_{3g}(3)$:	$Q(3) = \frac{1}{\sqrt{2}}[(-x_1 - y_1) + (x_2 + y_2) + (x_3 + y_3) + (-x_4 - y_4)]$	F^c	$e(3) \sim -a_3Q(1) + b_3Q(3)$
$B_{3g}(4)$:	$Q(4) = \frac{1}{\sqrt{2}}[(x_1 - y_1) + (x_2 - y_2) + (-x_3 + y_3) + (-x_4 + y_4)]$	K	$e(4) \sim Q(4)$
$B_{3g}(5)$:	$Q(5) = \frac{1}{\sqrt{2}}[(-x_1 - y_1) + (x_2 + y_2) + (x_3 + y_3) + (-x_4 - y_4)]$	K	$e(5) \sim Q(5)$

both the end members. Similar weak extra lines are reported in $Rb_2Cr_xMn_{1-x}Cl_4$ [15]. We think the extra lines originate from very small clusters of CuF_6 which are distorted differently from those in the samples with larger x. A report concerning these extra lines will be published elsewhere.

Acknowledgments

The authors are grateful to Professors M Hidaka, T Nakayama and Y Natsume for their continued help and advice.

References

[1] Totani M, Fukada Y and Yamada I 1989 *Phys. Rev.* B **40** 10577
[2] Kaneko M, Kuwabara G and Misu A 1976 *Solid State Commun.* **18** 1085
[3] Borovik-Romanov A S, Kreines N M, Laiho R, Levola T and Zhotikov V Z 1980 *J. Phys. C: Solid State Phys.* **13** 879
[4] Natsume Y and Yamada I 1983 *Solid State Commun.* **47** 839; 1985 *J. Phys. Soc. Japan* **54** 4410
[5] Riley M J, Dubicki L, Moran G, Krausz E R and Yamada I 1990 *Inorg. Chem.* **29** 1614; 1990 *Chem. Phys.* **145** 363
[6] Jamet J P, Ferré J and Yamada I 1987 *J. Phys. C: Solid State Phys.* **20** 3571
[7] Okuda Y, Tohi Y, Yamada I and Haseda T 1980 *J. Phys. Soc. Japan* **49** 936
[8] Yamada I, Shimoda S and Nagano S 1983 *Physica* B **121** 127
[9] Hidaka M, Inoue K, Yamada I and Walker P J 1983 *Physica* B **121** 343
[10] Bürger H, Strobel K, Geick R and Müller-Lierheim W 1976 *J. Phys. C: Solid State Phys.* **9** 4213
[11] Strobel K and Geick R 1976 *J. Phys. C: Solid State Phys.* **9** 4223
[12] Strobel K and Geick R 1982 *J. Phys. C: Solid State Phys.* **15** 2105
[13] Lehner N, Rauch H, Strobel K, Geick R, Heger G, Bouillot J, Renker B, Rousseau M and Stirling W G 1982 *J. Phys. C: Solid State Phys.* **15** 6545
[14] Catlow C R A, Diller K M and Norgett M J 1977 *J. Phys. C: Solid State Phys.* **10** 1395
[15] Moch P, Abdalian A T, Dugantier C, Briat B and Nerrozi M 1983 *J. Physique Coll. Suppl.* **49** C8 1503